Relaxation of the adsorption geometry of Sb and K on Si(001) surface induced by an electric field

Anna Pomyalov
Department of Chemical Physics, Weizmann Institute of Science, Rehovot, 76100, Israel
(Received 20 May 1997; revised manuscript received 11 November 1997)

The electric field-induced relaxation of the adsorption geometry of Sb and K atoms on Si(001)2×1 surface was studied using *ab initio* cluster calculations. We have found that the adsorption geometry changes considerably due to field. The difference in the response to the applied field of the different adatoms and the underlying Si layer is remarkable. The relaxation of the Sb dimer is less than that of the clean surface dimers, whereas the changes in K atom positions are an order of magnitude larger than those of the clean surface. In addition, there are drastic changes in the geometry of the Si dimers on the K-covered surface. The buckling of the dimers increases greatly for a positive field; for a negative field the increase in buckling is smaller. In both surfaces the relaxation of the Si dimers, to which the adsorbed atom is bonded, is defined by the elastic interactions with the adsorbed atom and differs from that of clean surface. The distribution of the field does not affect significantly the changes in adsorption geometry. However, for the field-sensitive surfaces, an extremely sharp tip may cause a selective desorption of the adsorbed atoms. [S0163-1829(98)01215-6]

I. INTRODUCTION

The adsorption of metals on a silicon surface has been a subject of study for already more than three decades (see, for example, reviews Refs. 1–4). Such a stable interest in the structure and properties of covered Si surfaces is dictated by their importance for both technological applications and fundamental research. The classical example of such a surface is the Si(001) surface. The complicated reconstructions developed on this surface provide a variety of adsorption sites. The site preferences and the actual adsorption geometry for different metals were studied both experimentally and theoretically.[1,4,5–11] With the invention of the scanning tunneling microscope (STM) a further step was taken in understanding the local structural and electronic properties of metal-semiconductor systems. These are especially important for adsorption at low coverage, for which the averaging techniques are insensitive. Nevertheless, there are discrepancies between the results obtained with different techniques and the calculated adsorption geometries.[10,12–17] The STM experiments on Si(001) surface are usually carried out with voltages around 2 V. The electric field induced by a biased tip is extremely strong, about 10^8 V/cm, which is of the order of the crystal field. In semiconductors the external field penetrates inside the bulk up to 0.5 μm. Therefore, one expects a pronounced effect of the field on the surface structure.

The effect of the electric field on the atomic and electronic structure was discussed for a clean Si(001) surface.[6,18–20] It was shown that an external electric field causes additional relaxation in the surface layer. As was estimated by Huang *et al.*[18] this relaxation is small. The elastic properties of the surface in the vicinity of an adsorbed atom, however, are different from that of the clean surface. The adsorption geometry, therefore, may be affected during the imaging process.

In the present work the problem of field sensitivity of the adsorption geometry of individual metal atoms on Si(001) surface is addressed. As an example two metals with a large difference in polarizability were used: Sb and K. The polarizability of a free Sb atom is close to that of Si, while it is much larger for K atoms. Both systems have been well studied experimentally and theoretically and are widely used in microelectronics.[6,8,9,12,14,16,21]

The Si(001) surface is reconstructed with the surface unit cell having the same size as in the bulk in one direction and twice as large in another [so-called Si(001)2×1 reconstruction].[19,22–24] This reconstruction was proposed on the basis of room-temperature low-energy electron diffraction (LEED) experiments in which a 2×1 diffraction pattern was observed. It is built of dimer rows running along the $[\bar{1}10]$ direction with dimers oriented in the [110] direction (see Fig. 1).

The dimerization reduces by half the number of dangling bonds. In the symmetric dimers they are half filled (Fig. 2). Further lowering of the surface energy can by achieved by a buckling of the dimers (a change in the relative height of two dimer atoms). The charge transfer between the upper and the lower dimer atoms leads to a filling of the lower dangling bond at the expense of the upper one. It is widely accepted that the dimers are asymmetric in their ground state. The symmetric dimers seen in STM images at room temperature are not static, but rather represent the time average of dynamically switching asymmetric dimers. The switching is ac-

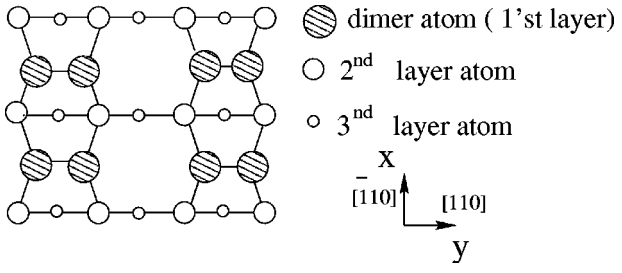

FIG. 1. Dimer model of the Si(001)2×1 surface: a top view.

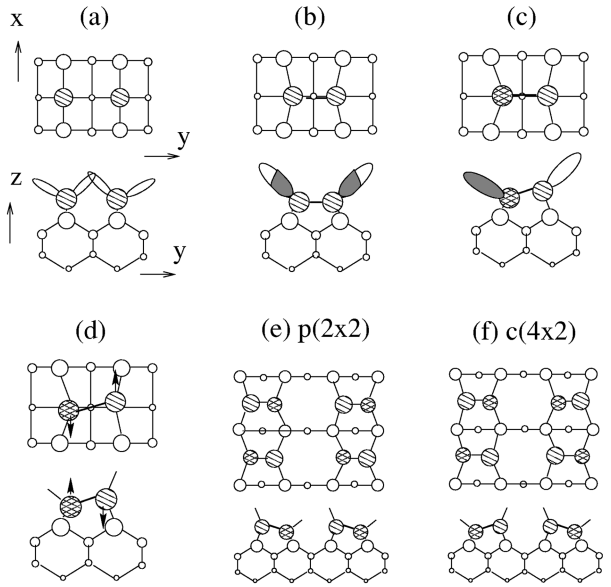

FIG. 2. Dimer model of the Si(001)2×1 surface: Top view (top) and side view (bottom) of (a) bulk-like terminated surface, (b) symmetric dimer, (c) asymmetric dimer. In (d) the switching and twisting directions are shown by arrows. The twisting directions are opposite for the adjusted dimers in the row. (e),(f) Formation of higher-order reconstructions. (e) $p(2\times2)$ in-phase buckling in the neighboring rows, (f) $c(4\times2)$ out-of-phase buckling in the neighboring rows. The orientation of x and y axes shown in panel (a) is the same as in Fig. 1.

companied by a slight twisting along the $[\bar{1}10]$ direction [Fig. 2(d)]. The asymmetric dimers are always buckled alternatively along the row. When the dimers in the neighboring rows are buckled ''in-phase,'' they produce the so-called $p(2\times2)$ reconstruction [Fig. 2(e)]. The ''out-of-phase'' buckling gives a $c(4\times2)$ reconstruction [Fig. 2(f)]. The latter structure is considered to be a minimum of the Si(001) surface, although the energy difference is very small (on the order of 0.01 eV per dimer). At room temperature the two structures are in thermal equilibrium and can be locally switched from one to the other by simultaneous flipping of two adjusted dimers from one row.

The adsorption of a foreign atom locally changes the dimers' structure. The new arrangement of dimers depends on the nature of the adsorbed atom-substrate interactions.

Antimony atoms at low coverage are thought to be adsorbed on Si(001) as dimers sitting on top of the Si dimer rows and oriented perpendicularly to the underlying Si dimers[8,9] (Fig. 3). These dimers are almost broken and the arrangement of Si atoms is close to that of the bulk-truncated surface.

Among different proposed adsorption sites for the adsorption of alkali metals (AM) on Si(001) (Fig. 3) the cave ($T4$) and the valley bridge ($T3$) sites are considered to be more stable than other sites.[5,10,12,13] Also of importance is the structure of the underlying Si dimers. Symmetrization of the dimers was proposed for saturation coverage[12,13] and is frequently used in the analysis of structural measurements for submonolayer coverage. However, Ko *et al.*[13] showed that for Na atoms adsorbed at low coverage, buckling of the surface dimers persists.

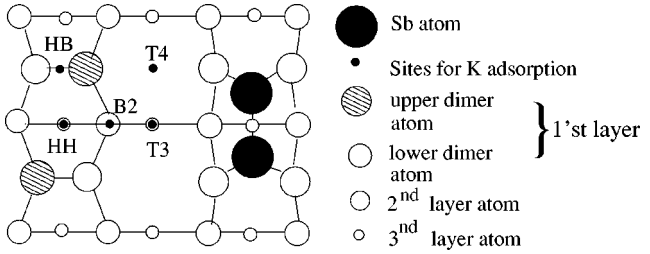

FIG. 3. The adsorption sites for Sb an K in Si(001) surface. $T4$, $T3$, HH, HB, and B2 denote the cave, valley bridge, pedestal, dimer bridge, and intermediate bridge sites, respectively.

These models of atomic adsorption were calculated as the lowest-energy configurations. In comparing such models with STM images the possible distortion of the adsorption geometry as a result of the tip-induced field was not taken into account. The existing discrepancies in the interpretation of STM images even for intensively studied semiconductor surfaces call for a better understanding of the influence of the electric field on the imaged surface.

In the present paper the results of *ab initio* cluster total-energy calculations of the field-induced relaxation of the adsorption geometry of Sb and K atoms on Si(001) surface are reported. It was found that the equilibrium position of adsorbed atoms significantly changes with the field. It was also shown that the relaxation of underlying surface dimers is not related to the electrostatic interaction with the external field, but rather to the elastic force applied by the relaxed adsorbed atom. The force constants corresponding to different bonds in the first surface layer of both surfaces and the effective force constants for adsorbed atoms have been calculated. The additional displacement and changes in the desorption barrier caused by a localized nonuniform field distribution (characteristic for the STM experiments) were estimated.

The paper is organized as follows. In Sec. II the model used in the calculations of the surface is described. In this section I specify the cluster structures, the field distribution, and the details of the computational procedure. In Sec. III the results for the field-induced changes in adsorption geometry are presented. In Sec. III A the surface response to a uniform electric field is discussed. The relaxation of the Si dimers in the vicinity of the adsorbed atom is explained using calculated bond force constants. In Sec. III B the effect of the nonuniform field component on the equilibrium position and the shape of the potential well for adsorbed atoms is discussed. In Sec. IV the findings are summarized.

II. MODEL

A. Surface model

In order to reproduce the details of the Si(001)2×1 reconstruction and to study the interaction between this surface and adsorbed atom one should be able to calculate the structural and electronic properties of the surface from first principles with high enough accuracy. *Ab initio* calculations involving a large number of atoms demand high computational resources and are very sensitive to the system size. The choice of the appropriate model for the surface is, thus, of great importance for the reliability of the calculations. In the present work the cluster model of the surface was adopted,

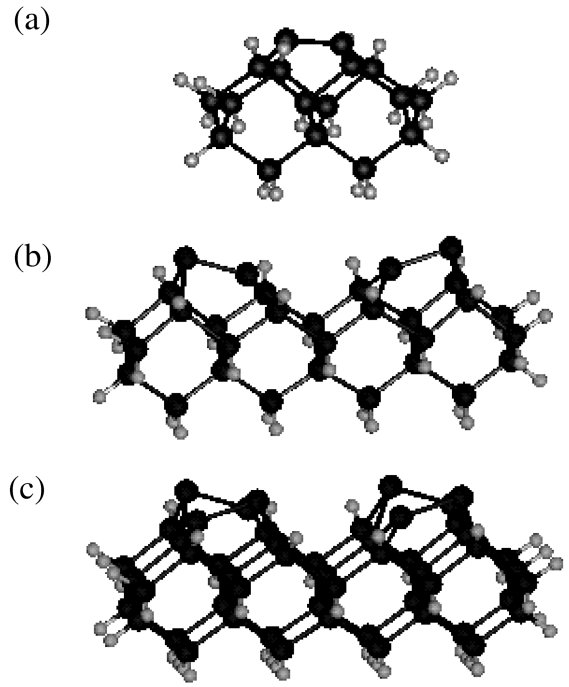

FIG. 4. Ball-and-stick models for the clusters representing the clean Si(001) surface. Panel (a): the one-dimer $Si_{17}H_{20}$. Panel (b): the double-dimer $Si_{31}H_{32}$. Panel (c): the four-dimer $Si_{53}H_{44}$.

since the exact geometry of a chemisorbed site was not known and a variety of structures had to be studied.

To define the appropriate clusters size the structure of the clean Si surface was calculated. The clean Si(001)2×1 surface was represented by clusters containing one dimer ($Si_{17}H_{20}$), two dimers from parallel rows ($Si_{31}H_{34}$), and four dimers ($Si_{53}H_{44}$), shown in Fig. 4. The parameters of the optimized cluster's geometry were reported in Ref. 25. All calculated atomic structures are in reasonable agreement with other calculations.[7,20,22,23] This allows me to use these clusters as a substrate and to proceed with a covered surface. To simulate the covered Si(001) surfaces a $Si_{15}H_{20}Sb_2$ cluster for a Sb/Si(001) surface was used. Our study of the relative stability of cave and valley bridge sites showed that the cave site for adsorption of K is the most stable one.[25] To represent the K/Si(001) surface a $Si_{31}H_{32}K$ cluster was used (Fig. 5). For all clusters asymmetric Si dimers were assumed as a starting geometry. All broken bonds (except the surface dangling bonds) were saturated with hydrogen atoms. Then, Si, Sb, and K atoms were allowed to relax to minimize the total energy of the cluster. Hydrogen atoms were fixed in their positions during geometry optimization to simulate the rigid bulk.

In the cluster geometry, C_{2V} symmetry was assumed to reduce the amount of calculations. The symmetry used restricted to some extent the geometry relaxation. A test study for large clusters using low symmetry (C_s and C_i) showed that this limitation does not significantly affect the results.

B. Tip model

The resolution of the STM images depends crucially on the tip. The ideal STM tip, giving the maximum resolution, is a point source of the current. A more realistic description

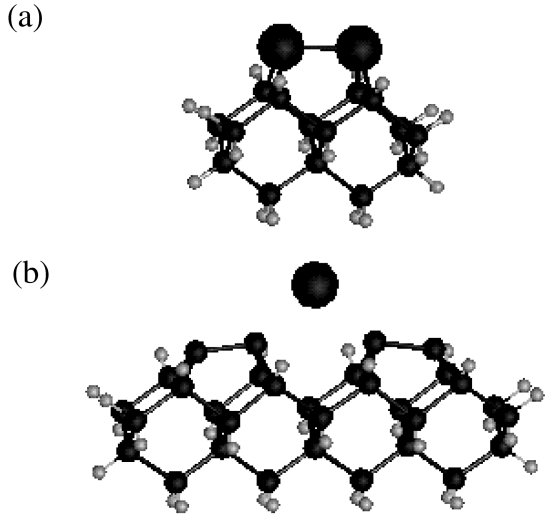

FIG. 5. Ball-and-stick models for the clusters representing the covered Si(001) surface. Panel (a): the $Si_{15}H_{20}Sb_2$ cluster representing the Sb/Si(001) surface. Panel (b): the $Si_{31}H_{32}K$ cluster representing the cave adsorption site in K/Si(001) surface.

should include the detailed tip structure. However, the actual atomic structure of the tip is usually unknown. An adequate tip model is, thus, dictated by the problem to be solved. In the present study the key quantity is the distribution of the electric field induced by a biased tip. It was shown[26,27] that, for this purpose, the STM tip can be considered as a metal plate with a small cluster on it. When bias voltage is applied between the tip and the sample, the body of the tip induces a uniform electric field E_0, which is defined by a macroscopic configuration of the tip-surface system. The small cluster causes an enhancement of the electric field just below it, whose spatial distribution as well as the magnitude are defined by the tip-sample geometry at the microscopic level. The field enhancement can be estimated as follows: A classically defined potential of a charged hemisphere on a conducting plane is given by

$$\Phi(\mathbf{r}) = -E_0 z\left(1-\frac{r_0^3}{r^3}\right), \tag{1}$$

where E_0 is the uniform field far from the hemisphere, r_0 is the radius of the hemisphere, $\mathbf{r}$ is measured from the center of the hemisphere, z is the direction perpendicular to the plate, and ρ is the direction parallel to the plate ($r^2=z^2+\rho^2$).

The z projection of the electric field is, thus, the z derivative of the potential $\Phi(\mathbf{r})$:

$$E_z(z,\rho) = E_0\left(1-\frac{r_0^3}{r^3}+\frac{3z^2r_0^3}{r^5}\right). \tag{2}$$

The field enhancement δ_0 below the hemisphere at a distance A is

$$\delta_0 = \left(\frac{E_z(A,\rho=0)-E_0}{E_z(A,\rho=0)}\right). \tag{3}$$

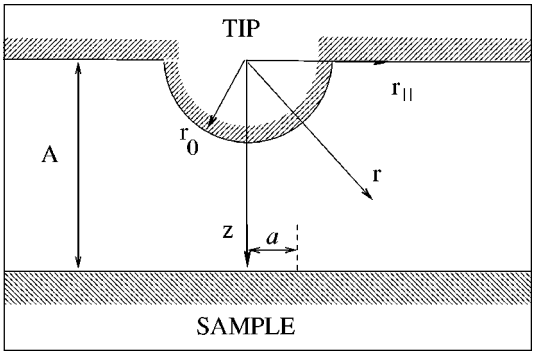

FIG. 6. Tip-sample geometry — the vacuum region.

The nonuniformity of the electric field δ_1 can be described by a lateral variation of the E_z on the interatomic distances a:

$$\delta_1 = \left(\frac{E_z(A,\rho=a) - E_z(A,\rho=0)}{E_z(A,\rho=0)} \right). \tag{4}$$

For the geometry shown in Fig. 6 $\delta_0 = (2r_0^3/A^3)/(1+2r_0^3/A^3)$, $\delta_1 = \delta_0[(1+4a^2/A^2)^{5/2} - 1 + a^2/2A^2)]/(1+4a^2/A^2)^{5/2}$.

There are two extreme cases:

1. $r_0 \approx A \gg a$ (blunt tip). For $r_0 = 10$ Å , $A = 15$ Å, $a = 5$ Å one finds $\delta_0 = 0.24$ and $\delta_1 = 0.01$. The field enhancement in the vicinity of the apex is not small, but can be considered as uniform. Therefore, the total field is $E_0 + \Delta E$, with ΔE constant.

2. $A \gg r_0 \approx a$ (the tip with a single atom at its apex). For $r_0 = 2.5$ Å, $a = 5$ Å, and $A = 7.5$ Å one finds $\delta_0 = 0.07$ and $\delta_1 = 0.09$. The field enhancement is nonuniform, but small and hence may be treated in the framework of the first-order perturbation theory with the perturbation potential $\phi(\mathbf{r}) = E_0 z r_0^3/r^3$.

The external electric field penetrates substantially into the semiconductor. To correctly estimate the electric field E_0 produced by the tip in the vacuum region, the buffering role of the semiconductor bulk should be considered. For a tunneling distance of 5 Å and a bias voltage of −1 V applied to n-type silicon without surface states with a doping level of 1×10^{18} cm^{-3}, E_0 is estimated as 0.12 V/Å.[25] Therefore, the relevant range of the electric fields induced in STM experiments on a Si(001) surface is $\pm 0.1 - 0.3$ V/Å.

C. Method of calculation

As already mentioned, the optimized geometry and energetic properties of the clusters should be calculated on an *ab initio* level. To this end, I used an *ab initio* all-electron numerical total-energy method, the so-called ''DMol,''[28–30] based on density-functional theory (DFT). The Hedin-Lundqvist/Janak-Morruzi-Williams local correlation[31] and the Becke gradient-corrected exchange functionals[32] were used. The convergence criterion was 1×10^{-6} Ry for the energy and 1×10^{-3} Ry/(a.u.) for the energy gradient. For all atoms, a double numerical basis set with a frozen-core approximation for the $1s2s$ orbitals of Si and the $1s2s2p$ orbitals of Sb and K was used. The integration grid for molecular orbitals was generated in a spherical pattern around each atomic center.[28,33] Radial integration points were taken from nucleus to an outer distance of 10 bohr. Angular integration points were generated at each of the radial points using Gaussian quadrature schemes.[34–36] In the present work the integration grid with about 1000 points per atom was used. The uniform external electric field was entirely included in the calculations of the self-consistent potential.

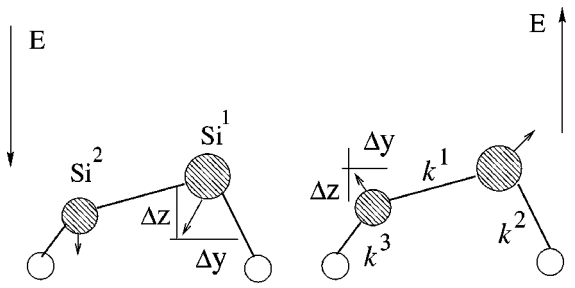

FIG. 7. The field-induced geometry relaxation of dimer atoms of the clean surface. Dimer atoms are shaded. Here and in Figs. 8 and 9, the direction of the field and atom displacement are shown by arrows. The bond force constants are indicated near the corresponding bond. Actual values of Δz and Δy for different fields are given in Table I, k is given in Table II.

III. FIELD-INDUCED GEOMETRY RELAXATION

A. Effect of the uniform field

To study the effect of an uniform external electric field on the geometry of the clean, Sb-, and K-covered Si(100) surfaces, the clusters were reoptimized in the presence of field of strength ± 0.1, ± 0.2, and ±0.3 V/Å. The field was applied normal to the surface, the positive direction pointing out of the surface.

It was found that the adsorption geometry significantly changes upon application of the field. The changes in the equilibrium position of the adsorbed atoms upon applied field were discussed in Ref. 25. The effect, however, is more complicated and involves also substrate atoms. The difference in the response to the applied field between the different adatoms and the underlying Si layer is remarkable (Figs. 7–9).

In the clean surface, the dimer atoms are shifted in the z and y directions (Fig. 7). The relaxation of both atoms is quite small, being larger for the upper dimer atom. It results in an increase of the dimer buckling for a negative field and a decrease for the positive. This small change in the dimer structure, however, results in charge transfer within the dimer.

The relaxation of the Sb dimer is asymmetric with respect to the field polarity. In the negative field both the Sb dimer and the underlying Si dimers are almost unaffected. In the positive field the Sb dimer is pulled out of the surface. The Si atoms are also shifted (Fig. 8). The Sb dimer bond and Sb-Si bond lengths slightly increase, whereas the distances between the first-layer Si atoms decrease. Changes in the Sb and Si positions are of the same order as in the clean surface surface.

As for the K/Si(001) surface, the changes in the K atom positions are an order of magnitude larger than those of the clean Si dimers. The asymmetry in the action of the fields of different polarities is also present. Unlike the clean Si(001)

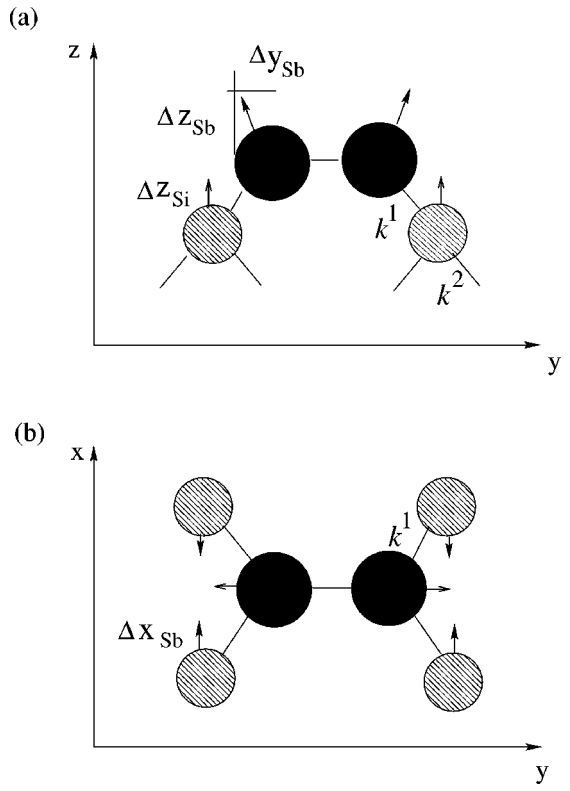

FIG. 8. The field-induced geometry relaxation of dimer atoms of the Sb/Si(001) surface for the positive field: (a) side view, (b) top view. Black circles denote Sb atoms, shaded circles denote Si atoms.

surface, the buckling of the dimers increases for both field polarities (Fig. 9). The K-Si and Si dimer bond lengths changed significantly with the field.

The direction of the relaxation for different atoms is shown in Figs. 7–9. Positive Δx, Δy, and Δz denote relaxation *out of the center* of the clusters, negative values denote relaxation *towards* the cluster center. The absolute values of the displacments are given in Table I.

One would expect the direction of the relaxation of the atoms to be defined by their effective charge. The upper dimer atom in the clean Si surface is negatively charged because of charge transfer in the buckled dimer. Sb and K atoms are positively charged. Although the charges change

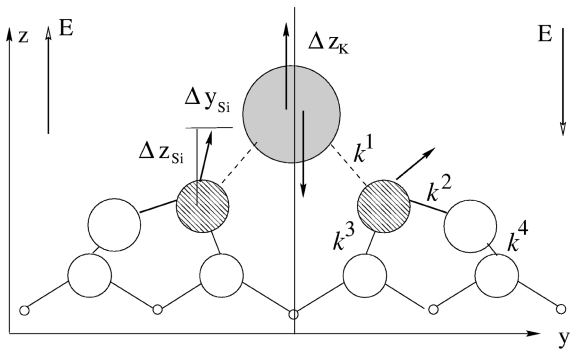

FIG. 9. The field-induced geometry relaxation of dimer atoms of the K/Si(001) surface. Large shaded circle denotes the K atom, small shaded circles denote the upper Si dimer atoms. Open circles denote Si atoms that do not move during relaxation.

TABLE I. The field-induced displacements for different atoms (in units of Å). Positive Δx, Δy, and Δz denote relaxation *out of the center* of the clusters, negative values denote relaxation *towards* the cluster center.

	E (V/Å)			
	−0.3	−0.2	0.2	0.3
Clean Si(001)				
Si^1 Δz	−0.05	−0.03	0.03	0.05
Δy	−0.03	−0.02	0.03	0.05
Si^2 Δz	−0.02	−0.01	0.01	0.02
Δy	0.01	0	−0.01	−0.02
Sb/Si(001)				
Sb Δz	0	0	0.03	0.05
Δy	0	0	0.01	0.02
Si Δz	0	0	0.01	0.02
Δx	0	0	−0.01	−0.02
K/Si(001)				
K Δz	−0.23	−0.17	0.22	0.41
Si^1 Δz	0.1	0.1	0.06	0.08
Δy	0.06	0.05	−0.03	−0.05

with the field, for these atoms, indeed, the direction is defined by the relative sign of the effective charge and the external field. For the underlying Si atoms, however, the direction and the magnitude of the displacement cannot be explained by a simple action of the electrostatic force.

To clarify this point I used the following procedure. First, the elastic properties of the surface in the vicinity of the adsorbed atoms were defined. The force constants for different bonds were calculated. To this end, the surface atoms were manually displaced (one atom at time) by $\Delta z = \pm 0.1$ Å from their equilibrium positions. Then the restoring forces acting on all atoms of interest were analyzed. The forces were calculated as gradients of the total energy. The procedure was repeated for both dimer atoms on a clean surface, the Sb dimer and underlying Si atoms, and the K atom with two dimer atoms (atoms related by symmetry were displaced together preserving the total symmetry of the cluster). The constants are listed in Table II.

Next, the forces induced by the electric field ± 0.2 V/Å in the zero-field structures were calculated. Then all atoms (except hydrogen atoms) were allowed to relax and the evolution of the forces induced on all atoms of interest was followed during geometry relaxation.

Consider first the adsorbed atoms. The external field induces significant forces on these atoms. The net displace-

TABLE II. The calculated bond force constants k (in units of eV/Å^2) for Sb/Si(001) and K/Si(001) surfaces. The bonds, to which the force constants correspond, are defined in Figs. 7–9.

Surface	k^1	k^2	k^3	k^4
Clean Si(001)	5.4	5.2	1.1	
Sb/Si(001)	4.8	5.4		
K/Si(001)	0.22	2.12	1.74	5.2

TABLE III. The calculated effective force constants k (in units of eV/Å^2) for different atoms.

	Clean Si(001)		Sb/Si(001)		K/Si(001)		
	Si^1	Si^2	Sb	Si	K	Si^1	Si^2
k^{eff}	5.2	5.4	5.1	5.4	0.25	2.2	5.2

ment is a result of the competition between the electrostatic force F_E and the restoring elastic forces F_k. The displacement is small for Sb ($\approx$0.03 Å). In contrast, for K even moderate electrostatic forces of about 0.05 eV/Å cause a displacement of 0.15–0.25 Å.

As for the underlying Si atoms, their relaxation is predominantly defined by the elastic interactions with displaced adatoms. For Sb/Si(001) it results in a small *upward* displacement of about 0.01 Å despite the effective negative charge of Sb atoms. The effect is especially pronounced for Si dimers in the K/Si(001) surface. Here, the dimer buckling increases for both polarities of the field due to the displacement of the Si^1 atom (see Table I and Figs. 8 and 9).

The electric-field-induced changes in the bond lengths and the relative height of the adsorbed atoms and the substrate affect the local electronic structure in the vicinity of the adsorbed atoms. As both the atomic and the local electronic structure of the surface contribute to the formation of the STM images, the appearance of the adsorbed atoms in images may be changed by the electric field. This effect has been discussed in detail elsewhere[25].

B. Sharp tip — the effect of the nonuniform field

The atomically resolved STM images can be obtained only with a sufficiently sharp tip. On the other hand, I have shown that the field distribution under such a tip is essentially nonuniform. To study the effect of the field gradient on the surface atomic and electronic structure, I used a model potential for a sharp tip defined in Sec. II B. The perturbation potential is well localized and quickly decreases with the distance. This allows me to use the same clusters as were used for the calculations with the uniform field, at least for a perturbation located close to the center of the cluster.

To estimate the possible changes in geometry caused by the nonuniform field component, I have evaluated the forces acting on different atoms due to distortion of the potential well. The potential surface of an atom near the equilibrium position can be described by a Hooke's law potential[37] $\psi = kz^2/2$ with the coefficient k set to the effective force constant of the corresponding atom. The effective force constants, including the contributions from all relevant bonds, were calculated using the bond force constants (see Table III).

Next, I checked whether the effective force constants of adsorbed atoms can be considered as field independent in the range of the fields used in this work. To evaluate the displacement Δz (caused by the uniform electric field E_0) I used the condition of mechanical equilibrium: $k_0 \Delta z = F_{el}(E_0)$. Here k_0 is the zero-field force constant and $F_{el}(E_0)$ is the force, applied to the unrelaxed atoms by the external field ± 0.2 V/Å. Then, the ''exact'' displacements were calculated using an *ab initio* geometry optimization.

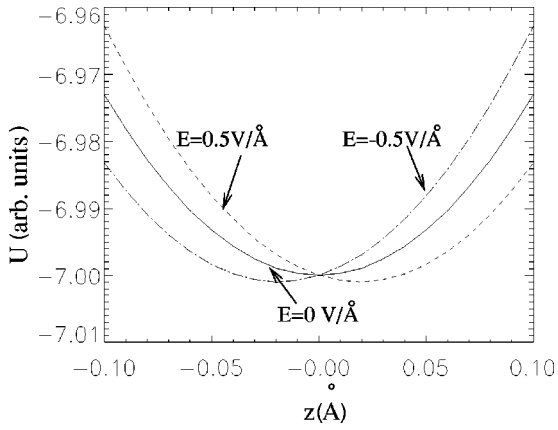

FIG. 10. The cross sections of $U(z,\rho)$ for a Si atom in a clean Si(001) surface (normal to the surface), which show dependence of the potential on the nonuniform electric field with an asymptotic strength $E_0 = \pm 0.5$ V/Å (solid line: no field, dotted line: $E_0 = 0.5$ V/Å, dashed line: $E_0 = -0.5$ V/Å).

The two displacements agree within 0.01 Å. Thus, in further analysis the zero-field force constants were used.

Using the calculated effective force constants, I have studied the dependence of the shape of the atomic potential on the nonuniform component of the electric field. Consider a Hooke's law potential in a nonuniform field:

$$U(\mathbf{r}) = U_0 + \frac{kr^2}{2} - qE_0 z\left(1 - \frac{r_0^3}{(r - r_0^{tip})^3}\right), \qquad (5)$$

where U_0 is an arbitrary chosen well depth, k is the effective force constant, q is the effective charge of the atom, E_0 is the uniform field strength, r_0 is the radius of the tip apex, and r_0^{tip} is the position of the apex center relative to the atom position. For a particular atom [characterized by k and $q(E_0)$] and a particular tip size and position, the shape of the potential surface depends only on the electric field strength E_0. Throughout this section I have used $r_0 = 2.5$ Å and $r_0^{tip} = 6.5$ Å.

The potential surface of both Si dimer atoms in the clean surface is only slightly tilted even by a relatively strong field (see Fig. 10). A small nonuniform field component hardly affects the atomic position for both polarities of the field.

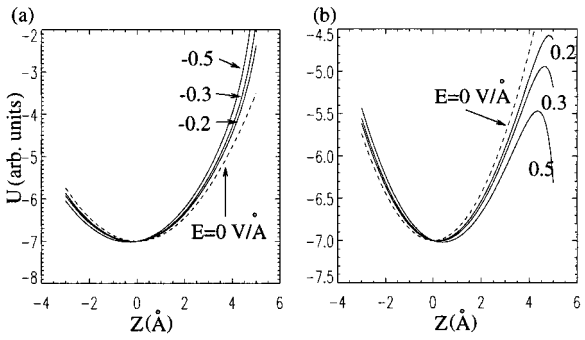

FIG. 11. The effect of the electric field on the potential for a Sb atom in the Sb/Si(001) surface. The cross sections of $U(z,\rho)$ for a negative field (a) and a positive field (b). Here, and in other figures, numbers correspond to strengths E_0 in the asymptotic region.

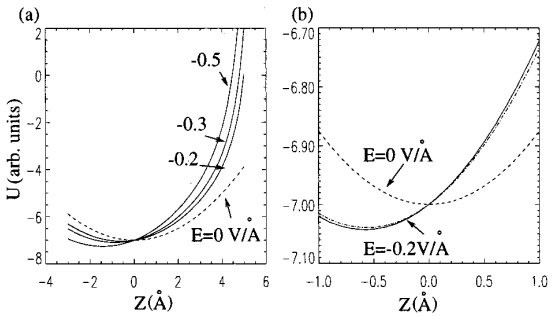

FIG. 12. The effect of a negative electric field on the potential for a K atom in the K/Si(001) surface. Panel (a): The cross sections of $U(z,\rho)$ normal to the surface, showing dependence of the potential on the nonuniform electric field. Panel (b): the cross sections of the potential surface for $E_0=-0.2$ V/Å (dotted line — no field; dashed line — uniform field $E_0=-0.2$ V/Å; dashed-dotted line — nonuniform field with an asymptotic strength $E_0=-0.2$ V/Å).

As I already mentioned there is an asymmetry in the action of the field for the Sb atoms. In the negative field the effect of the small nonuniform component of the field is negligible. The equilibrium position is the same for both the uniform and nonuniform fields. In the positive field [Fig. 11(b)] the desorption barrier is lowered, but the potential surface near the equilibrium point is still hardly affected.

The K atom is the most sensitive, as was found in the case of a uniform field. There is a strong asymmetry in its response to fields of different polarities. In the negative field (Fig. 12) the equilibrium point is shifted towards deeper z with increasing field and the potential barrier for desorption increases. Nevertheless, the shift of the equilibrium point is small even for a strong field (-0.5 V/Å). On the other hand, an increasing positive field (Fig. 13) lowers the barrier for desorption. A field of the order of $+0.5$ V/Å opens an escape channel for the atom. Thus, a sudden increase of the tip-induced field may cause selective desorption of the K atom. In the normal operation regime of the STM ($E\approx 0.2$ V/Å), the changes in the equilibrium point position are small [Fig. 13(d)].

Such a small displacement can be estimated using the simplified potential [Eq. (5)]. To this end, I calculated the gradient of this potential at position z, corresponding to the equilibrium position of the atom in the uniform field $E_0=\pm 0.2$ V/Å. The resulting displacements are negligible

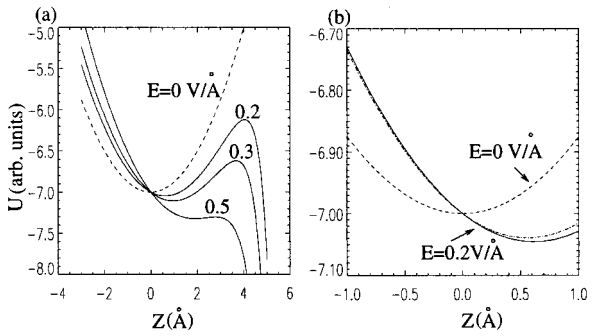

FIG. 13. The same as in Fig. 12, for K atom in the K/Si(001) surface in the positive field.

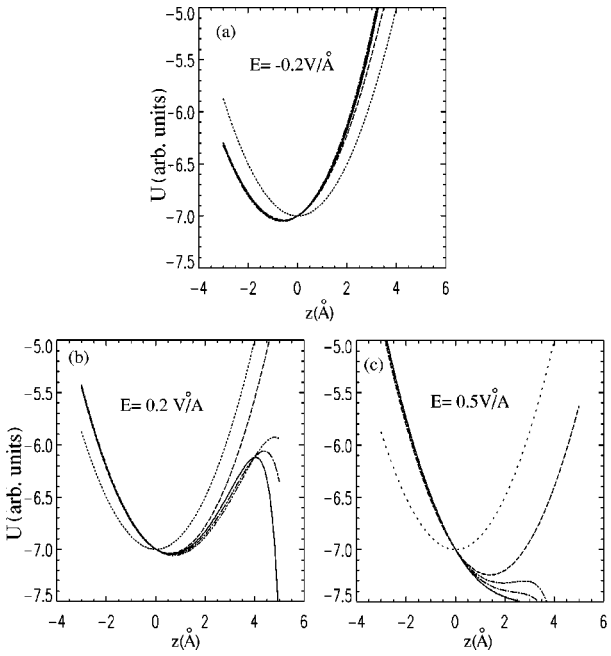

FIG. 14. The effect of the apex size on the potential well for a K atom in K/Si(001) surface. The cross sections of $U(z,\rho)$ (normal to the surface) in the nonuniform field are shown with an asymptotic strength (a) $E_0=-0.2$V/Å, (b) $E_0=0.2$ V/Å, (c) $E_0=0.5$V/Å. In each panel, a dotted line denotes a zero-field surface; dashed line: $r_0=\infty$; solid line: $r_0=2.5$ Å; dashed-dotted line: $r_0=3.7$ Å; dashed-dot-dot line: $r_0=5.0$ Å.

for clean Si and Sb/Si(001) surfaces. For K/Si(001) the additional displacement is also small: -0.01 Å for -0.2 V/Å and $+0.03$ Å for $+0.2$ V/Å.

To illustrate the effect of the apex size on the equilibrium position of an adsorbed atom, I used an example of K/Si(001) (Fig. 14). As shown in Sec. II B, the nonuniform field distribution approaches that of the uniform field upon increasing the apex radius. For a negative field [Fig. 14(a)] the apex size does not affect much the potential shape. However, for a positive field, the effect is significant [Fig. 14(b) and 14(c)]. The desorption barrier increases with increasing r_0, even for a strong field (0.5 V/Å). The equilibrium position is shifted towards its position in the uniform field $E_0+\Delta E$ (see Sec. II B).

IV. CONCLUSION

In the present work, I have explicitly accounted for the electric-field-induced relaxation of the atomic structure in covered Si surfaces. It was found that the adsorption geometry of Sb and K on a Si(001) surface is significantly affected by the external electric field. The relaxation of the Si dimers in the vicinity of the adsorbed atoms was found to be governed by elastic interaction with the displaced adsorbed atom, and differs from relaxation of the clean Si surface. The force constants corresponding to different bonds and the effective force constants for adsorbed atoms were calculated.

The uniformity of the field distribution (defined by the size of the STM tip) does not affect significantly the changes in adsorption geometry. However, for the field-sensitive surfaces, an extremely sharp tip may cause a selective desorption of the adsorbed atoms.

ACKNOWLEDGMENTS

I am grateful to V.S. L'vov for numerous fruitful discussions during the preparation of the manuscipt. The author also wishes to thank Yishay Manassen, who has drawn my attention to the usefulness of simple mechanical analogies in the language of force constants for the discussion of surface relaxation. This work was supported by the Minerva Foundation, Munich, Germany, by a grant from the Basic Investigation Foundation administered by the Israeli Academy of Sciences and Humanities, and by the Edith Reich Fund.

[1] R. I. G. Uhrberg and G. V. Hansson, Crit. Rev. Solid State Mater. Sci. **17**, 133 (1991).
[2] H.N. Waltenburg and Y. T. Yates, Chem. Rev. **95**, 1589 (1995).
[3] F. J. Himpsel, Surf. Sci. Rep. **12**, 1 (1990).
[4] H. Neddermeyer, Rep. Prog. Phys. **59**, 701 (1996).
[5] I. P. Batra, Phys. Rev. B **43**, 12 322 (1991), and references therein.
[6] Y. Hasegawa, I. Kamiya, T. Hashizume, T. Sakurai, H. Tochihara, M. Kubota, and Y. Murata, Phys. Rev. B **41**, 9688 (1990).
[7] L. Spiess, P. S. Mangat, S.-P. Tang, K. M. Schirm, A. J. Freeman, and P. Soukiassian, Surf. Sci. Lett. **289**, L631 (1993).
[8] M. Richter *et al.*, Phys. Rev. Lett. **65**, 3417 (1990).
[9] Y. W. Mo, Phys. Rev. Lett. **69**, 3643 (1992).
[10] Y. Ling, A. J. Freeman, and B. Delley, Phys. Rev. B **39**, 10 144 (1989).
[11] T. Kendelewicz, P. Soukiassian, R. S. List, J. C. Woicik, P. Pianetta, I. Lindau, and W. E. Spicer, Phys. Rev. B **37**, 7115 (1988).
[12] K. Kobayashi, Y. Morikawa, K. Terakura, and S. Blugel, Phys. Rev. B **45**, 3469 (1992).
[13] Y.-J. Ko, K.J. Chang, and J.-Y. Yi, Phys. Rev. B **51**, 4329 (1995).
[14] R. Souda, W. Hayami, T. Aizawa, and Y. Ishizawa, Phys. Rev. B **47**, 9917 (1993).
[15] M. K.-J. Johansson, S. M. Gray, and L. S. O. Johansson, Phys. Rev. B **53**, 1362 (1996).
[16] H. Ishida and K. Terakura, Phys. Rev. B **40**, 11 519 (1989).
[17] L. S. O. Johansson and B. Reihl, Surf. Sci. **287/288**, 524 (1993); Phys. Rev. B **47**, 1401 (1993).
[18] Z.-H. Huang and R. E. Allen, Ultramicroscopy **42-44**, 97 (1992); Z.-H. Huang, M. Weimer, R. E. Allen, and H. Lim, J. Vac. Sci. Technol. A **10**, 974 (1992).
[19] P. Badziag and W. S. Verwoerd, Surf. Sci. **285**, 145 (1993); P. Badziag, W. S. Verwoerd, and M. A. van Hove, Phys. Rev. B **43**, 2058 (1991).
[20] M. M. D. Ramos, A. M. Stoneham, and A. P. Sutton, J. Phys.: Condens. Matter **5**, 2849 (1993).
[21] A. Brodde, Th. Bertrams, and H. Neddermeyer, Phys. Rev. B **47**, 4508 (1993).
[22] I. P. Batra, Phys. Rev. Lett. **43**, 11 140 (1995).
[23] S. Tang, A. J. Freeman, and B. Delley, Phys. Rev. B **45**, 1776 (1992).
[24] A. I. Shkrebti, R. D. Felice, C. M. Bertoni, and R. Del Sole, Phys. Rev. B **51**, 11 201 (1995).
[25] A. Pomyalov and Y. Manassen, Surf. Sci. **382**, 275 (1997).
[26] D. J. Rose, J. Appl. Phys. **27**, 215 (1956).
[27] H. J. Kreuzer, L. C. Wang, and N. D. Lang, Phys. Rev. B **45**, 12 050 (1992).
[28] B. Delley, J. Chem. Phys. **92**, 508 (1990).
[29] B. Delley, J. Chem. Phys. **94**, 7245 (1991).
[30] DMol, Biosym Technologies, San Diego.
[31] L. Hedin and B. I. Lundquist, J. Phys. C **4**, 2064 (1971).
[32] A. D. Becke, Phys. Rev. A **38**, 3098 (1988).
[33] A. D. Becke, J. Chem. Phys. **88**, 2547 (1988).
[34] A. H. Stroud, *Approximate Calculation of Multiple integrals* (Prentice-Hall, Englewood Cliffs, NJ, 1971).
[35] V. I. Lebedev, Zh. Vychisl. Mat. Mat. Fiz. **15**, 48 (1975); V. I. Lebedev, *ibid.* **16**, 293 (1977).
[36] S. I. Konyaev, Mat. Zametki **25**, 629 (1979).
[37] L. Pauling and E. B. Wilson, *Introduction to Quantum Mechanics* (McGraw-Hill Book Company, Inc., New York, 1935), Pt. 1.